ZnSe:Mn/ZnS quantum dots for the detection of microcystin by room temperature phosphorescence immunoassay

Jiaqi You[1], Long Ma[1], Yu He[1,2] ✉, Yili Ge[1], Gongwu Song[1], Jiangang Zhou[2]

[1]*Hubei Collaborative Innovation Center for Advanced Organic Chemical Materials, Ministry-of-Education Key Laboratory for the Synthesis and Application of Organic Functional Molecules, College of Chemistry and Chemical Engineering, Hubei University, Wuhan 430062, People's Republic of China*
[2]*Hubei Province Key Laboratory of Regional Development and Environment Response, Wuhan 430062, People's Republic of China*
✉ *E-mail: heyu@hubu.edu.cn*

Published in Micro & Nano Letters; Received on 25th November 2018; Revised on 5th March 2019; Accepted on 26th March 2019

This work has assembled ZnSe:Mn/ZnS quantum dots (QDs)-monoclonal anti-microcystin-Leucine Arginine (anti-MC-LR) antibody bioconjugates as a room temperature phosphorescence (RTP) probe using 1-ethyl-3-(3-dimethyllaminopropyl) carbodiimide/N-Hydroxysuccinimide chemistry for detecting MC-LR. Once the specific interactions occurred between these MCs and their antibodies on the surface of ZnSe:Mn/ZnS QDs, the RTP of ZnSe:Mn/ZnS QDs was quenched with the increased concentration of MC-LR. Under the optimised conditions, the linear range of MC-LR was determined to be 0.9–8.8 nM. The linear relationship between $(P_0–P)/P_0$ and concentration of MC-LR were observed with the regression equation $(P_0–P)/P_0 = 0.03908C + 0.0456$ with the detection limit of 0.038 nM. The developed RTP immunoassay favoured environmental applications since the interference from autofluorescence and scattering light was greatly eliminated.

1. Introduction: The frequent occurrence of cyanobacteria blooms in eutrophic water bodies has become a serious environmental problem in the world [1]. In addition, this issue is often associated with the production of microcystin (MC), a toxic secondary metabolite in the surrounding aquatic ecosystem [2, 3]. MCs pose a serious threat to aquatic organisms, drinking water safety and human health through food chain accumulation [4, 5]. Particularly, MC-Leucine Arginine (MC-LR) is considered as the most toxic and common in the family of MCs [6]. The World Health Organisation has set the maximum allowable standard concentration of MC-LR in drinking water as 1 μg l^{-1} in light of the ubiquity contamination and its strong toxicity [7, 8]. The content of MC-LR in water has been used as an important standard indicator of water quality by many countries and organisations. Therefore, the development of new methods for detecting MC-LR has captured great interest [9].

The analytical techniques for MC in aquatic environment mainly involve chromatographic techniques [10–12], liquid–liquid microextraction [13], enzyme-linked immunosorbent assay [14, 15], quantum dot (QD) labelling [16], recombinant plant-based antibodies [17], capillary electrophoresis [18] and protein phosphatase inhibition assay [7, 19]. However, the relatively expensive equipment, high testing costs and complicated pretreatment processes limit the development of these methods [20]. Therefore, there is an urgent need to develop a simple, sensitive and easy-to-use method that can specifically detect MC-LR in water.

Due to the unique optical properties of semiconductor QDs, it has been widely used in many fields especially as luminescence probe [21]. Mn doped ZnS QDs have been explored as the room temperature phosphorescence (RTP) probe due to its advantages, such as the wider gap between the excitation and emission spectra, the longer emission lifetime, anti-interference from autofluorescence and the scattering light of the matrix [22–25]. The ZnSe:Mn/ZnS QDs have been synthesised for better chemical stability and higher RTP intensity in their potential applications of phosphorescence sensing and imaging [26].

Taking the advantage of RTP detection and immunorecognition, we employed water-soluble ZnSe:Mn/ZnS QDs as the RTP probe for the trace detection of MC-LR (Fig. 1). First, we synthesised water-soluble Mn: ZnSe QDs and made ZnS shell grow on its surface to obtain water-soluble ZnSe:Mn/ZnS QDs that emit orange-red phosphorescence. Then the ZnSe:Mn/ZnS QDs was covalently linked by monoclonal anti-MC-LR antibody. Once the specific interactions occurred between these MC-LR and their antibodies on the surface of ZnSe:Mn/ZnS QDs, the RTP of ZnSe:Mn/ZnS QDs was quenched with the increased concentration of MCs. Therefore, we established a simple, sensitive, selective and applicable method for the detection of MC-LR.

2. Experimental

2.1. Reagents: All chemicals were at least of analytical grade. Selenium powder (99.9%), 3-mercaptopropionic acid (MPA) (98%), 1-ethyl-3-(3-dimethyllaminopropyl) carbodiimide hydrochloride (EDC) (98%) and N-Hydroxysuccinimide (NHS) (98%) were purchased from Aladdin Reagent Co., Ltd. (Shanghai, China). Manganese acetate, 1-octadecene (ODE, 90%), oleylamine (OLA) and oleic acid were purchased from Macklin Biochemical Co., Ltd. (Shanghai, China). Zinc acetate, thiourea, sodium borohydride (98%) and cyclohexane were purchased from Sinopharm Chemical Reagent Co., Ltd. (Shanghai, China). MC-LR monoclonal antibody was obtained from Suwei Microbe Co., Ltd. (Wuxi, China). MC-LR standard solutions were purchased from Taiwan Algal Science Inc.. MC-LF, MC-LY, MC-LA, MC-YR and MC-RR were from Enzo Life Sciences, Inc. (Switzerland). Phosphate buffer solution (PBS) (pH = 7.2) was purchased from Solarbio Science & Technology Co., Ltd. (Beijing, China).

2.2. Apparatus: Transmission electron microscopy (TEM) images were obtained on a Tecnai G20 microscope (FEI, USA). High resolution transmission electron microscopy (HR TEM) images were performed on JEM-2100UHR STEM/EDS (JEOL, Japan). High performance liquid chromatography (HPLC) UltiMate 3000 were purchased from Dionex China Co., Ltd. The phosphorescent intensity was recorded on a LS55 fluorescence spectrometer (Perkin-Elmer, USA).

doi: 10.1049/mnl.2018.5690

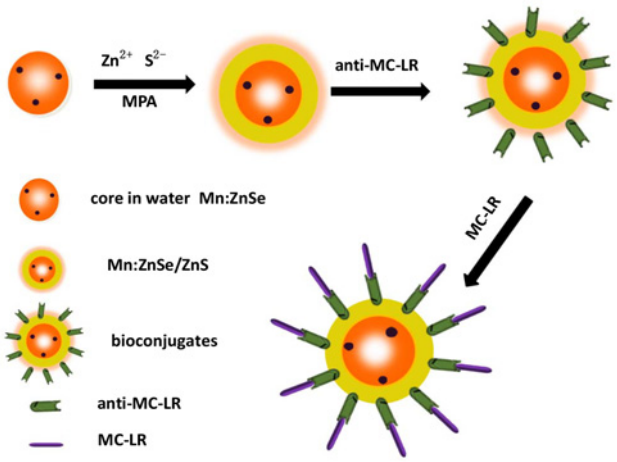

Fig. 1 *Schematic illustration for fabricating ZnSe:Mn/ZnS QDs for RTP detection of MC-L*

2.3. Preparation of water-soluble ZnSe:Mn/ZnS core/shell QDs: The precursor solutions were prepared according to the reference with little modification [26]. 1 mM zinc acetate was dissolved in 3 ml of OLA and 15 ml of toluene to form zinc precursor solution after heating at 85°C. 0.03 mM manganese acetate was dissolved in 1.5 ml of toluene and 0.5 ml of OLA to form manganese precursor solution after heating at 85°C. For the preparation of NaHSe, 2 mM of $NaBH_4$ and 1 mmol of selenium powder were added to 2 ml of ultrapure water. After reacting for 40 min at 4°C, the black selenium powder disappeared and a transparent NaHSe solution was obtained.

First, 1 ml of oleic acid, 1 ml of ODE, the as-prepared manganese and zinc precursor solution were loaded into an autoclave. Subsequently, 15 ml of fresh NaHSe aqueous solution was added into the above mixture with stirring for 10 min and sealed at 120°C for 1.5 h. Then and oil-soluble ZnSe:Mn cores in the toluene were separated from the crude solution after the autoclave was cooled down to room temperature. Finally the oil-soluble ZnSe:Mn cores were dispersed in cyclohexane and stored for further use.

The ZnSe:Mn cores in cyclohexane were treated with MPA solution by shaking for 20 min to form the MPA-coated ZnSe:Mn precipitate. The precipitate was transferred into the aqueous solution with pH 12 by continuous stirring. Then, ZnSe:Mn cores were further protected by ZnS shell employing MPA as the capping agents. The A fresh aqueous solution (10 ml) containing 1 mmol zinc acetate and 10 mmol MPA were added into 80 ml of ZnSe:Mn colloidal solution by stirring under pH = 12. The thickness of ZnS shell was controlled by the amount of additional precursors (zinc acetate and thiourea, Zn/S = 1:1 molar ratio). After stirring for 30 min, 10 ml of thiourea was added into the solution (molar ratio of Zn/S = 1:1). The mixture was heated to 95°C and was continuously stirred for 3 h, then the ZnSe:Mn/ZnS QDs were obtained.

2.4. Synthesis of ZnSe:Mn/ZnS QDs-monoclonal anti-MC-LR antibody bioconjugates: Bioconjugates were synthesised based on previous references [27], 4.5 mg of ZnSe:Mn/ZnS QDs were dissolved in 3 ml of 10 mmol l^{-1} PBS (pH = 7.2), followed by addition of 200 µl of 4 mg ml^{-1} EDC, with stirring at room temperature for 10 min. After that 200 µl of 0.15 mg ml^{-1} NHS was added and the mixture was stirred at room temperature for 20 min. Finally, 200 µl of 0.01 mg ml^{-1} monoclonal anti-MC-LR antibodies were added for incubating for 2 h at 37°C. The mixture was purified by centrifugation at 8000 rpm for 5 min with using a 100-KD ultrafiltration tube to finally obtain ZnSe:Mn/ZnS QDs-monoclonal anti-MC-LR antibody bioconjugates and stored in the fridge at 4°C for further use.

2.5. Sensitivity of bioconjugates for MC-LR detection: The detection of MC-LR was carried out in PBS buffer solution (pH 7.2, 10 mM) at room temperature. First, 10 µl of MC-LR standard solution with different concentrations was added to the ZnSe:Mn/ZnS QDs-monoclonal anti-MC-LR antibody bioconjugates (600 µl), respectively (final concentrations of MC-LR: 0, 0.9, 1.7, 2.5, 3.7, 4.8, 5.5, 6.5, 7.1, 7.5, 8.3, 8.8 nM). Then the RTP of the samples were measured. The excitation wavelength of 330 nm was used and the slit widths of the excitation and emission were both set to 15 nm. The percentage of RTP quenching after the bioconjugates incubate with MC-LR was used for quantitative measurement.

3. Results and discussion

3.1. Influence on the RTP properties of ZnSe:Mn/ZnS QDs: First, we synthesised ZnSe:Mn core by the phase-interface solvothermal method. Then the ZnS shell was deposited on ZnSe:Mn core in aqueous solution to obtain the ZnSe:Mn/ZnS QDs. The Mn luminescence can be controlled by changing the thickness of ZnS shell and the doping concentration of Mn.

The RTP of the ZnSe:Mn/ZnS QDs were illustrated in Fig. 2. As shown in Fig. 2*a*, strong phosphorescence emission was observed at 580 nm (black curve) due to the well-known $^4T_1$–$^6A_1$ transition at an excitation wavelength of 330 nm (Red curve) [28, 29]. It was noteworthy that the RTP intensity of the oil-soluble ZnSe:Mn QDs was weak, which was due to surface defects and oxidation of the surface Se (Fig. 2*b*). After the oil-soluble ZnSe:Mn was transferred to the aqueous solution the samples still showed weak Mn emission. After the ZnS shell was deposited on the ZnSe:Mn cores, the RTP intensity of ZnSe:Mn/ZnS was significantly increased. The inset of Fig. 2*b* is corresponding to ZnSe:Mn/ZnS QDs dispersed in water before and after excitation at 365 nm under UV lamp. The thickness of the shell tended to play a critical role in the phosphorescence intensity of QDs. As shown in Fig. 2*c*, when the ZnSe:Mn was coated with a layer of ZnS shell, the phosphorescent intensity of ZnSe:Mn/ZnS QDs was sharply increased because the coated ZnS shell not only isolated the QDs from the surrounding environment but also reduced the probability of non-irradiative transitions. Further coating of ZnS shell decreased the

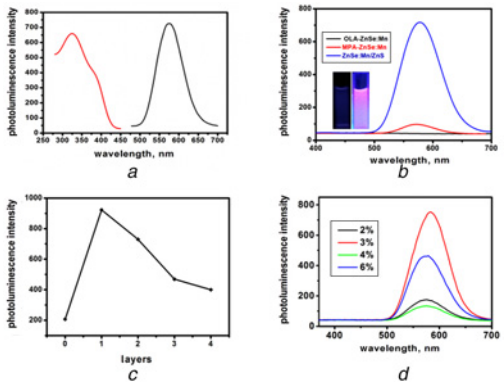

Fig. 2 *Phosphorescence spectra and optimal synthetic conditions for ZnSe:Mn/ZnS QDs*
a Phosphorescence excitation and emission spectra of the ZnSe:Mn/ZnS QDs
b Phosphorescence emission spectra of original OLA-capping ZnSe:Mn cores, MPA-capping ZnSe:Mn cores in the aqueous solution and ZnSe:Mn/ZnS QDs. The inset of *b* corresponds to ZnSe:Mn/ZnS QDs dispersed in water before and after excitation at 365 nm under UV lamp
c Phosphorescence intensity of ZnSe:Mn/ZnS QDs influenced by the different layers of ZnS
d Phosphorescence intensity of ZnSe:Mn/ZnS QDs influenced by the doping concentration of Mn

phosphorescent intensity of ZnSe:Mn/ZnS QDs due to the lattice mismatch between the ZnS shell and the ZnSe, thereby increasing the defects in the crystal and increasing the non-radiative transition channels [30, 31]. The amount of doped Mn also affected the phosphorescence intensity of ZnSe:Mn/ZnS QDs. When the Mn^{2+} doping concentration was 3%, the RTP intensity of ZnSe:Mn/ZnS QDs reached the maximum.

3.2. Characterisation of the ZnSe:Mn/ZnS QDs: The TEM and HRTEM images of the ZnSe:Mn QDs and ZnSe:Mn/ZnS QDs are displayed in Figs. 3*a* and *b*. The images reveal that the ZnSe:Mn QDs are nearly monodispersed with an average diameter of 4.3 nm (Fig. 3*a* and inset of Fig. 3*a*). Compared to the ZnSe:Mn/ZnS QDs with an average diameter of 4.8 nm, the increase of core/shell particle size was about 0.54 nm (Fig. 3*b* and inset of Fig. 3*b*).

As shown in Fig. 4, the effect of the concentration of ZnSe:Mn/ZnS QDs on the RTP intensity of bioconjugates was discussed. The RTP intensity of the bioconjugates increased as the concentration of ZnSe:Mn/ZnS QDs varied from 0.25–1.5 mg/ml, then levelled off from 1.5–2 mg/ml. Furthermore, increase in the concentration of ZnSe:Mn/ZnS QDs decreased the quenched phosphorescence intensity. Therefore, the concentration of the ZnSe:Mn/ZnS QDs with 1.5 mg/ml was chosen in further study.

3.3. Feasibility of the ZnSe:Mn/ZnS QDs-monoclonal anti-MC-LR antibody bioconjugates as the RTP probe for the detection of MC-LR: To evaluate the feasibility of ZnSe:Mn/ZnS QDs-monoclonal anti-MC-LR antibody bioconjugates for the detection of MC-LR, the experiment was designed to detect MC-LR in PBS buffer (pH 7.2, 10 mM) at room temperature. Fig. 5*a* shows no RTP response of the Mn-doped ZnS QDs (1.5 mg/ml) to MC-LR in aqueous solution. After the conjunction with anti-MC-LR antibody, the RTP intensity of ZnSe:Mn/ZnS QDs-monoclonal anti-MC-LR antibody bioconjugates displayed a regular decrease as the concentration of MC-LR increased (Fig. 5*c*). Therefore, we established the RTP immunoassay for the detection of MC-LR. We investigated the incubation time on the

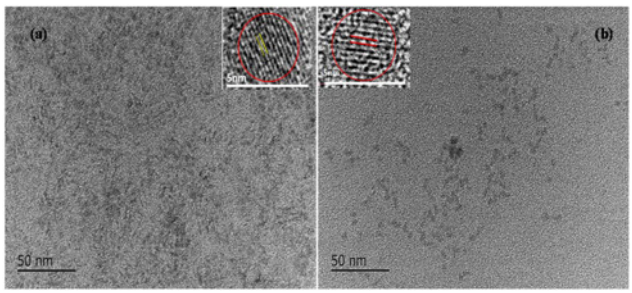

Fig. 3 *TEM and HRTEM image*
a TEM and HRTEM image of the ZnSe:Mn core
b TEM and HRTEM image of the ZnSe:Mn /ZnS QDs

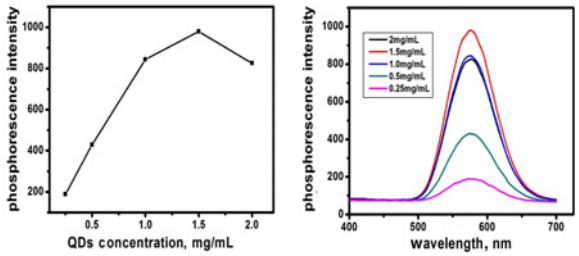

Fig. 4 *Effect of the concentration of QDs on the RTP intensity of bioconjugates*

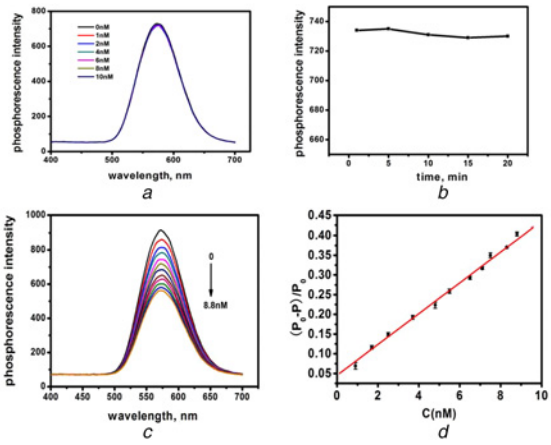

Fig. 5 *The detection of MC-LR*
a Effect of MC-LR on phosphorescence quenching percentage when added to core–shell QDs
b Effect of incubation time on the phosphorescence quenching percentage of bioconjugates when MC-LR was added
c RTP spectra of the QDs-bioconjugates on addition of different concentrations of MC-LR (from top to bottom: 0, 0.9, 1.7, 2.5, 3.7, 4.8, 5.5, 6.5, 7.1, 7.5, 8.3, and 8.8 nM
d Linear plots for (*c*)

RTP immunoassay for the detection of MC-LR (Fig. 5*b*). When the bioconjugates incubated with MC-LR from 0 to 20 min, the quenched RTP intensity kept unchanged, indicating that the bioconjugates incubated with MC-LR instantaneously. The linear range of MC-LR was determined to be 0.9–8.8 nM, the linear relationship between $(P_0–P)/P_0$ and C_{MC-LR} was observed with the regression equation $(P_0–P)/P_0 = 0.03908C + 0.0456$ (where C_{MC-LR} was in nM, $R^2 = 0.9955$, Fig. 5*d*), with the detection limit of 0.038 nM. Comparison with many other approaches to the MC-LR assay are shown in Table 1, indicating that the detection limits and the linear ranges were better or comparable to the previous works.

3.4. Selectivity of the QDs-bioconjugates for MC-LR detection: Selectivity is a very important parameter to evaluate the QDs-bioconjugates for MC-LR detection. Therefore, we choose the analogues of MC-LR including MC-RR, MC-LR, MC-LY, MC-LF, MC-LA that were introduced into the assay under optimised conditions. As shown in Fig. 6, five types of toxins were tested using this detection system at a concentration of two times higher than MC-LR (2 nM). The RTP intensity was obvious, changed only in presence of MC-LR. These results indicate that the QDs- bioconjugates probe is only selective for MC-LR.

3.5. Application of QDs-bioconjugates for the determination of MC-LR in real water samples: In order to explore the potential application of the proposed method, we was carried out to detect

Table 1 Comparison of the linear range and detection limit for MC-LR using different probes

Reagents	Analytical range, nM	Detection limit, nM	References
QD detection probe	0.42–25	0.0300	[32]
IC-ELISA	0.3–10	0.1000	[33]
ab-CdTe-based ICTS	0.25–5	0.1000	[34]
Fe_3O_4@Au magnetic nanoparticle	0.79–12.9	0.3800	[35]
recombinant antibody	0.21–5.9	0.1900	[36]
naYF4:Yb	0.1–50	0.0250	[37]
our method	0.9–8.8	0.0375	This paper

doi: 10.1049/mnl.2018.5690

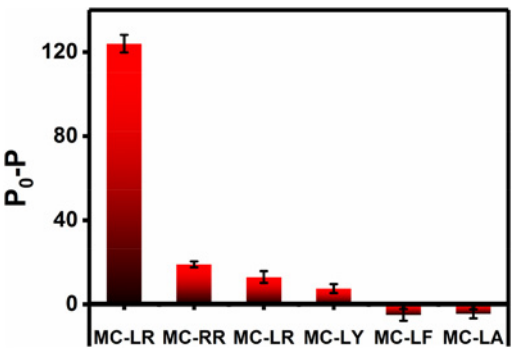

Fig. 6 *Selectivity of QDs-bioconjugates for MCs detection*

Table 2 Analytical results for actual water samples ($n = 3$)

Our method			
samples	Spiked, nM	Found, nM	Recover ± RSD, %
Yangze River water	8.300	7.652	92.2 ± 2.8
East lake water	16.60	15.17	91.4 ± 4.9
tap water	8.300	7.870	94.0 ± 5.2
HPLC Method			
samples	Spiked, nM	Found, nM	Recover ± RSD, %
Yangze river water	8.300	7.813	94.1 ± 1.8
East lake water	16.60	16.85	102 ± 1.1
tap water	8.300	7.903	95.2 ± 4.6

the concentration of MC-LR in actual water samples. Lake water samples were obtained from East Lake in Wuhan. River water was obtained from Yangzte River in Wuhan. The water samples were filtrated before use. The analytical results of MC-LR in water samples are summarised in Table 2. The recoveries of spiked MC-LR ranged from 91.4 to 94.0%, and the relative standard deviation (RSD) were no more than 5.20%, which illustrate the validity of the developed method. HPLC method as shown in Table 2, MC-LR was concentrated 1000 times. The conditions of HPLC were set as follows: an isocratic mobile phase consisted of methanol and water (0.05% trifluoroacetic acid) at a ratio of 55:45 and at a flow rate of 1 ml/min. The temperature of the chromatographic column (C_{18} column 250 mm × 4.6 mm ID, 5 µm particle size) was 25°C, and the wavelength of the UV detector was 238 nm [27]. After filtrated with 0.22 µm membrane filter, 20 µl of pretreated sample solution was injected.

4. Conclusion: In summary, a new QDs-bioconjugates-based RTP immunoassay was demonstrated and used for the specific determination of MC-LR in water samples. The obtained bioconjugate not only provided good performance for the detection of MC-LR, but also favoured environment applications because the phosphorescent detection mode avoided the interference from autofluorescence and scattering light from the water matrix. The developed probe displays relative high sensitivity, good selectivity, low-cost instrumentation. These merits make it promising to be used in routine analysis having more opportunities for application in environmental systems.

5. Acknowledgments: This work was financially supported by the National Natural Science Foundation of China (grant no. 21707030) and Wuhan Youth Science and technology plan (grant no. 2016070204010133).

6 References

[1] Ma J.G., Li Y.Y., Duan H.Y, *ET AL.*: 'Chronic exposure of nanomolar MC-LR caused oxidative stress and inflammatory responses in HepG2 cells', *Chemosphere*, 2017, **92**, pp. 305–317

[2] Wiegand C., Pflugmacher S.: 'Ecotoxicological effects of selected cyanobacterial secondary metabolites: a short review', *Toxicology Appl. Pharmcology*, 2005, **203**, pp. 201–218

[3] Perri K.A., Sullivan J.M., Boyer G.L.: 'Harmful algal blooms in Sodus Bay, Lake Ontario: a comparison of nutrients, marina presence, and cyanobacterial toxins', *J. Gt. Lakes Res.*, 2015, **41**, pp. 326–337

[4] Hu Y.X., Shang F., Liu Y., *ET AL.*: 'A label-free electrochemical immunosensor based on multi-functionalized graphene oxide for ultrasensitive detection of microcystin-LR', *Chem. Pap.*, 2018, **72**, pp. 71–79

[5] Li J.M., Cao L.R., Yuan Y, *ET AL.*: 'Comparative study for microcystin-LR sorption onto biochars produced from various plant-and animal-wastes at different pyrolysis temperatures: influencing mechanisms of biochar properties', *Bioresource Technol.*, 2018, **247**, pp. 794–803

[6] Min B.H, Ravikumar Y., Lee D.H., *ET AL.*: 'Age-dependent antioxidant responses to the bio concentration of microcystin-LR in the mysid crustacean,neomysis awatschensi', *Environ. Pollut.*, 2018, **232**, pp. 284–292

[7] Catanante G., Espin L., Marty J.L.: 'Sensitive biosensor based on recombinant PP1 alpha for microcystin detection', *Biosens. Bioelectron.*, 2015, **67**, pp. 700–707

[8] Eissa S., Ng A., Siaj M., *ET AL.*: 'Label-free voltammetric aptasensor for the sensitive detection of microcystin-LR using graphene-modified electrodes', *Anal. Chem.*, 2014, **86**, pp. 7551–7557

[9] Zhao C., Hu R., Liu T., *ET AL.*: 'A non-enzymatic electrochemical immunosensor for microcystin-LR rapid detection based on Ag@MSN nanoparticles', *Colloid. Surf. A.*, 2016, **490**, pp. 336–342

[10] Beltrán E., Ibáñez M., Sancho J.V., *ET AL.*: 'Determination of six microcystins and nodularin in surface and drinking waters by on-line solid phase extraction-ultra high pressure liquid chromatography tandem mass spectrometry', *J. Chromatogr.A.*, 2012, **1266**, pp. 61–68

[11] Kaloudis T., Zervou S.K., Tsimeli K.: 'Determination of microcystins and nodularin (cyanobacterial toxins) in water by LC-MS/MS. Monitoring of Lake Marathonas, a water reservoir of Athens, Greece', *J. Hazard, Mater.*, 2013, **263**, pp. 105–115

[12] Kim I.S., Nguyen G.H., Kim S.J., *ET AL.*: 'Qualitative analysis of the most toxic and abundant microcystin variants (LR, RR, and YR) by using LCMS-IT-TOF', *J. Ind. Eng. Chem.*, 2015, **29**, pp. 375–381

[13] Yu H.L., Clark K.D., Anderson J.L.: 'Rapid and sensitive analysis of microcystins using ionic liquid-based in situ dispersive liquid-liquid microextraction', *J. Chromatogr. A*, 2015, **1406**, pp. 10–18

[14] Reverte L., Garibo D., Flores C., *ET AL.*: 'Magnetic particle-based enzyme assays and immunoassays for microcystins: from colorimetric to electrochemical detection', *Environ. Sci. Technol.*, 2013, **47**, (1), pp. 471–478

[15] Heussner A.H., Winter I., Altaner S., *ET AL.*: 'Comparison of two ELISA-based methods for the detection of microcystins in blood serum', *Chem-Bool. Interact.*, 2014, **223**, pp. 10–17

[16] Yu H.W., Kim I.S., Niessner R., *ET AL.*: 'Multiplex competitive microbead-based flow cytometric immunoassay using quantum dot fluorescent labels', *Anal. Chim. Acta*, 2012, **750**, pp. 191–198

[17] Melnik S., Neumann A.C., Karongo R., *ET AL.*: 'Cloning and plant-based production of antibody MC10E7 for a lateral flow immunoassay to detect [4-arginine] microcystin in freshwater', *Plant Biotechnol. J.*, 2018, **16**, pp. 27–38

[18] Brothier F., Pichon V.: 'Immobilized antibody on a hybrid organic-inorganic monolith: capillary immunoextraction coupled on-line to nanoLC-UV for the analysis of microcystin-LR', *Anal. Chim. Acta*, 2013, **792**, pp. 52–58

[19] Sassolas A., Catanante G., Fournier D., *ET AL.*: 'Development of a colorimetric inhibition assay for microcystin-LR detection: comparison of the sensitivity of different protein phosphatases', *Talanta*, 2011, **85**, pp. 2498–2503

[20] Hou L., Ding Y.H., Zhang L.L., *ET AL.*: 'An ultrasensitive competitive immunosensor for impedimetricdetection of microcystin-LR via antibody-conjugated enzymaticbiocatalytic precipitation', *Sensor Actuat-B.*, 2016, **233**, pp. 63–70

[21] Freeman R., Willner I.: 'Optical molecular sensing with semiconductor quantum dots (QDs)', *Chem. Soc. Rev.*, 2012, **41**, (10), pp. 4067–4058

[22] Tang D.D., Zhang J.Y., Zhou R.X., *ET AL.*: 'Phosphorescent inner filter effect-based sensing of xanthine oxidase and its inhibitors with Mn-doped ZnS quantum dots', *Nanoscale*, 2018, **10**, (18), pp. 8477–8482

[23] Diaz-Diestra D., Thapa B., Beltran-Huarac J., *ET AL.*: 'L-cysteine capped ZnS:Mn quantum dots for room-temperature detection of dopamine with high sensitivity and selectivity', *Biosens, Bioelectron.*, 2017, **87**, pp. 693–700
[24] Deng P., Lu L.Q., Tan T., *ET AL.*: 'Novel phosphorescent Mn-doped ZnS quantum dots as a probe for the detection of L-tyrosine in human urine', *Anal. Methods*, 2017, **9**, pp. 287–293
[25] Wu P., Zhang J.Y., Yan X.P.: 'Progress of room temperature phosphorescent sensing application based on manganese-doped zinc sulfide quantum dots', *Chinese J. Anal. Chem.*, 2018, **45**, (12), pp. 1831–1837
[26] Dong B.H., Cao L.X., Su G., *ET AL.*: 'Facile synthesis of highly luminescent water-soluble ZnSe:Mn/ZnS core/shell doped nanocrystals with pure dopant emission', *J. Phys. Chem.C.*, 2012, **116**, (22), pp. 12258–12264
[27] Zhou X.P., Meng Y.H., Ma H.B., *ET AL.*: 'Method for determination of microcystin-leucine-arginine in water samples based on the quenching of the fluorescence of bioconjugates between CdSe/CdS quantum dots and microcystin-leucine-arginine antibody', *Microchim. Acta*, 2011, **173**, pp. 259–266
[28] Jin Q., Hu Y.L., Sun Y.X., *ET AL.*: 'Room-temperature phosphorescence by Mn-doped ZnS quantum dots hybrid with Fenton system for the selective detection of Fe^{2+}', *RSC Adv.*, 2015, **5**, pp. 41555–41562
[29] Jin Q., Li Y., Huo J.Z., *ET AL.*: 'The 'off–on' phosphorescent switch of Mn-doped ZnS quantum dots for detection of glutathione in food, wine, and biological samples', *Sensor Actuat. B-Chem.*, 2016, **227**, pp. 108–116
[30] Louver Y., Biadala L., Trebbia J.B., *ET AL.*: 'Efficient biexciton emission in elongated CdSe/ZnS nanocrystals', *Nano. Lett.*, 2011, **11**, (10), pp. 4370–4357
[31] Yang Y.A., Chen O., Angerhofer A., *ET AL.*: 'On doping CdS/ZnS core/shell nanoerystals with Mn', *Am. Chem. Soc.*, 2008, **130**, (46), pp. 15649–15661
[32] Yu H.W., Jang A., Kim L.H., *ET AL.*: 'Bead-based competitive fluorescence immunoassay for sensitive and rapid diagnosis of cyanotoxin risk in drinking water', *Environ. Sci. Technol.*, 2011, **45**, (18), pp. 7804–7811
[33] Sheng J.W., He M., Shi H.C.: 'A highly specific immunoassay for microcystin-LR detection based on a monoclonal antibody', *Anal. Chim.Acta.*, 2007, **603**, (1), pp. 111–118
[34] Sun J.D., Li Y., Pi F.W., *ET AL.*: 'Using fluorescence immunochromatographic test strips based on quantum dots for the rapid and sensitive determination of microcystin-LR', *Anal. Bioanal.Chem.*, 2017, **409**, (8), pp. 2213–2220
[35] Zhang J., Kang T., Sun R.X.: 'An immunosensor for microcystins based onFe3O4@Au magnetic nanoparticle modified screen-printed electrode chin', *J. Anal. Chem.*, 2013, **41**, pp. 1353–1358
[36] Murphy C., Stack E., Krivelo S., *ET AL.*: 'Detection of the cyanobacterial toxin, microcystin-LR, using a novel recombinant antibody-based optical-planar waveguide platform', *Biosens. Bioelectron.*, 2015, **67**, pp. 708–714
[37] Wu S.J., Duan N., Zhang H., *ET AL.*: 'Simultaneous detection of microcysin-LR and okadaic acid using a dual fluorescence resonance energy transfer aptasensor', *Anal. Bioanal. Chem.*, 2015, **407**, (5), pp. 1303–1312

doi: 10.1049/mnl.2018.5690